마이크로 모터의 자동화된 FEA 시뮬레이션

이준성*

Automated FEA Simulation of Micro Motor

Lee, Joon-Seong

Abstract

This paper describes an automated evaluation of electrostatic field for micro motors whose sizes range 10 to 10^3μm. Electric field modeling in micro motors has been generally restricted to in-plane two-dimensional finite element analysis (FEA). In this paper, the actual three-dimensional geometry of the micro motor is considered. An automatic FE mesh generation technique, which is based on the fuzzy knowledge processing and computational geometry techniques, is incorporated in the system, together with one of commercial FE analysis codes and one of commercial solid modelers. The system allows a geometry model of concern to be automatically converted to different FE models, depending on physical phenomena to be analyzed, electrostatic analysis and stress analysis and so on. The FE models are then exported to the FE analysis code, and then analyses are performed. Then, analytical analysis and FE analysis about the torque generated by electrostatic micro motor are performed. The starting torque is proportional to V^2, the calculated starting torque from the two-dimensional analytical solutions are three times larger than those from the three-dimensional FE solutions.

Key Words: Finite Element Analysis, Micro Motor, Fuzzy Knowledge Processing, Computational Geometry, Electrostatic Analysis, Starting Torque

* 경기대학교 전자·기계공학부

1. Introduction

Micromachines are extremely novel artifacts with a variety of special characteristics. Utilizing their tiny dimensions ranging roughly from 10 to 10^3micro-meters, the micromachines can perform tasks in a revolutionary manner that would be impossible for conventional artifacts[1]. Designing micromachines is (a) multi-disciplinary, (b) strongly interactive among design subprocesses such as design specification, conceptual design and detail design, (c) it also requires designers living in the macroscopic world to have very different empirical knowledge being valid in the microscopic world. Micromachines are in general related to various coupled physical phenomena.

In accordance with dramatical progress of computer technology, numerical simulation methods such as the Finite Element Method (FEM) are recognized to be key tools in practical designs and analyses. Computer simulations allow us for the testing of new designs without time-consuming and considerable efforts to experiments at every iteration process.

Fabrication of the actuators depends on micromachining techniques developed for semi-conductor devices. A number of efforts have been made so far to build electrostatic micro actuators[2-4]. However, most of the micro actuators have failed to generate enough force for practical applications. Therefore, a new concept of micro actuator is demanded.

In general, to estimate electrostatic performances of micro actuators, electrostatic field modeling has been restricted to in-plane two-dimensional FE analysis because of the complexity of actual micro actuator geometry [5].

The present author has proposed an automatic FE mesh generation scheme for three-dimensional complex geometry[6]. The author has integrated this mesh generator, commercial FE analysis code MARC[7] and commercial solid modeler Designbase[8] into a novel simulation system for micro-machines.

2. Electrostatic Micro Motor

The actuator most commonly used in the macro world is the ubiquitous electric actuator which is, in fact, an electromagnetic actuator. While this actuator is successful in producing large scale motions, it is poorly suited to small mechanisms that produce small motions. Electrostatic forces are well suited as an actuation force for small, micro-scale devices.

In this paper, the micro motor is conducted as a part of positioning device. This motor force uses an electrostatic force as other micro actuators do, and its fabrication process is almost the same as those in Ref.[3,4].

Its basic structure is shown in Figure 1. Figure 1(a) is its schematic plane view, and 1(b) is its cross-section view. The micro motor comprises a movable ring, i.e. rotor, four beams, and a plurality of electrodes, i.e. stator. Dimensions of its initial design are as follows. The ring is a ring-like plate of approximately 420 μm in outer diameter and 380 μm in inner diameter. The four beams are disposed at the inner space of the ring, and connect the ring with a substrate. The electrodes are provided in the circumferential region around the ring, and are larger than

the outer diameter of the ring by 5 μm to play the same roles as ordinary electrostatic micro motors.

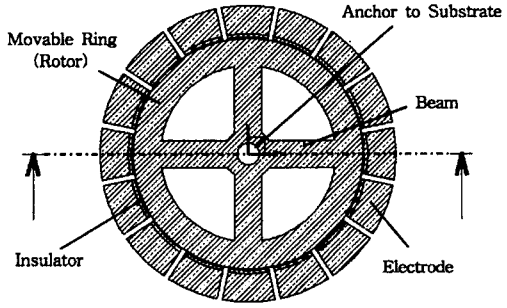

(a) Top View

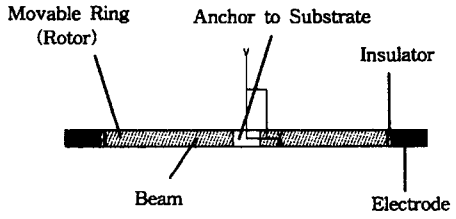

(b) Cross section view

Figure 1. Structure of micro motor

As illustrated in the left figure of Figure 2, when one of the electrodes is excited, the ring will be electrostatically attracted and come into contact with the insulating layers on the inner circumference of the electrode and the outer circumference of the ring. Then as illustrated in the right figure, as voltages are applied sequentially to the electrodes, the ring will revolve in the direction of the arrow, being attracted by the excited electrodes in succession.

However, since the ring and the electrodes move at the same time while both are in rolling contact with each other at the common contact point, the ring will rotate by the difference between the inner circumference laid out by the electrodes and the outer diameter of the ring. The rotation of the ring is in the direction of the arrow, which is opposite to the direction of its revolution.

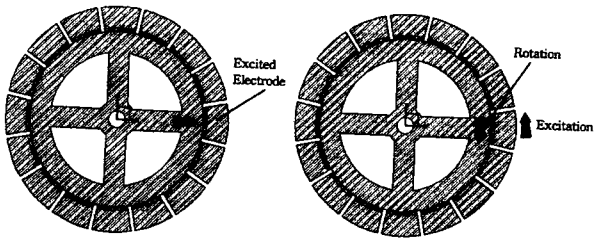

Figure 2. Motion of micro motor

As each electrode is excited sequentially, although the ring is fixed in position to the substrate by means of the beam anchor, the ring rolls inside of the electrodes once without slipping, it has transversed a distance greater than its own circumference. Conversely, upon removing the excitation from the electrodes even while the ring is in motion, the ring can be returned readily to the initial position on account of the rebounding force of the elastically deformed beams. Although the rotation of the ring is limited by the spiral beams, the actuator has several advantages such as high torque and low friction. This electrostatic micro motor is to be used as a micro-positioner.

3. Analytical Solution of Starting Torque

The theoretical analysis and FE analysis about the generated torque by electrostatic micro motor are performed. The particular dimensions of the actuator are shown in Table 1.

Table 1. Reference dimensions

Diameter of plane ring	420 μm
Thickness of plane ring	30 μm
Inner diameter of electrodes	427 μm
Thickness of spoke beams	30 μm
Width of spoke beams	40 μm
Thickness of insulator	2 μm

The electrostatic energy stored between the rotor and an electrode is calculated; then, the change in this energy as the rotor moves is determined. The change in energy is used to calculate the torque and output energy of the motor.

As shown in Figure 3, the radius of the rotor is r_r, the radius of the stator is r_s, the angular position of the electrode center is θ, and the electrode subtends an angle of θ_E from the center of the stator. In this figure, the rotor has been moved to the right until it touches an insulating layer of thickness t_i on the stator.

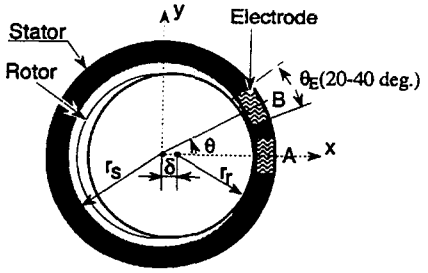

Figure 3. A diagram of the rotor and stator, showing radii, angles of the rotor

To calculate the energy stored between the electrode and rotor, the separation, d, between the electrode and rotor needs to be represented as a function of θ. First the intercept of the line at angle θ and the rotor (and similarly for the stator) is calculated, and then the separation, d, between these points on the rotor and stator. The distance between the rotor and stator, d, is

$$d=\sqrt{(x_s-x_r)^2+(y_s-y_r)^2} \quad (1)$$

Now part of this gap, d, between the rotor and stator is filled with an insulator of thickness ti, and the rest is filled with air. If the relative permittivity of the insulator is ε_i, then the effective distance[4] between the rotor and stator, d_E, is

$$d_E=d-t_i\left(\frac{\varepsilon_i-1}{\varepsilon_i}\right) \quad (2)$$

The potential energy stored in the capacitor formed by the rotor and electrode is now calculated.

$$U=\frac{1}{2}CV^2=\frac{\varepsilon_0 wt\,V^2}{2\,d_E} \quad (3)$$

where ε_0 is the dielectric constant of the vacuum, w is the width of the electrode, t is the thickness of the electrode, and V is the applied voltage to the electrodes.

There are two different angles associated with this actuator as shown in Figure 4. One of the advantages of this actuator is the large ratio that can be obtained between θ and Φ. The angle Φ is the angle of rotation of the rotor, and the θ is the angle to the energized electrode. That is, the distance from the electrode A to B is the same distance from C to D of the rotor by the contact point. The ratio of θ to Φ is given as follows :

$$r_r(\theta+\phi) = r_s\theta \tag{4}$$

$$\frac{\theta}{\phi} = \frac{r_r}{r_s - r_r} \tag{5}$$

The torque can be expressed as

$$\tau = \frac{dU}{d\phi} = \frac{dU}{d\theta} \cdot \frac{d\theta}{d\phi} = \frac{dU}{d\theta} \cdot \frac{r_r}{r_s - r_r} \tag{6}$$

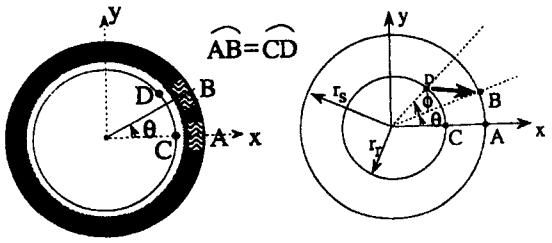

Figure 4. Motion of the micro motor

To use equation (6) to calculate the torque, the electrostatic potential energy between the electrode and rotor must be calculated. As shown in Figure 5, the width of the electrode is w and subtends an angle of θ_s to θ_e at the center of the stator. The gap between the rotor and stator is varied. The incremental energy dU is expressed as follows :

$$dU = \frac{\varepsilon_0 t V^2}{2 d_E} dw = \frac{\varepsilon_0 t V^2}{2 d_E} r_s d\theta \tag{7}$$

where $dw = r_s d\theta$ is the incremental length along the electrode.

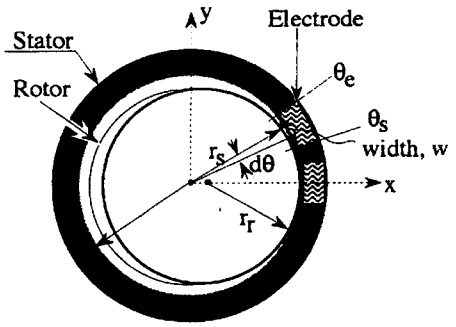

Figure 5. The electrode of width, w and thickness, t, is broken into elements $r_s d\theta$ in order to integrate for total electrostatic energy

The integral of the increments $r_s d\theta$, from the start of the electrode θ_s, to the end of the electrode θ_e, gives the total energy, U :

$$U = \int_{\theta_s}^{\theta_e} dU = \int_{\theta_s}^{\theta_e} \frac{\varepsilon_0 t V^2 r_s}{2 d_E} d\theta \tag{8}$$

where d_E is the function of θ.
From the above,

$$\tau = \frac{dU}{d\theta} \frac{r_r}{(r_s - r_r)}$$
$$= \left[\frac{r_r}{r_s - r_r}\right] \frac{d}{d\theta}\left[\frac{\varepsilon_0 t V^2 r_s}{2}\right] \int_{\theta_s}^{\theta_e} \frac{1}{d_E} d\theta$$
$$= \left[\frac{r_s}{r_s - r_r}\right]\left[\frac{\varepsilon_0 t V^2 r_s}{2}\right]\left(\frac{1}{d_E} \Big|_{\theta_e} - \frac{1}{d_E} \Big|_{\theta_s}\right) \tag{9}$$

Considering the insulator, the starting torque is eventually calculated as follows :

$$\tau = \left[\frac{r_s}{(r_s - t_i) - r_r}\right]\left[\frac{\varepsilon_0 t V^2 r_s}{2}\right]\left(\frac{1}{d_E} \Big|_{\theta_e} - \frac{1}{d_E} \Big|_{\theta_s}\right)$$

To find the torque, only the values of d_E at the ends of the electrode need to be known.

4. FEA System

The developed system allows designers to evaluate detailed physical behaviors of structures through some simple interactive opreations to their geometric models. In other word, designers do not have to deal with mesh data when they operate system.

4.1 Definition of geometry model

A whole analysis domain is defined using commercial geometry modeler Designbase, which has abundant libraries to be easily operated, modified and referred to a geometry model. Any information related to a geometry model can be easily retrieved using those libraries.

4.2 Attachment of Material Properties and Boundary Conditions to Geometry Model

Material properties and boundary conditions are directly attached onto the geometry model by clicking the loops or edges that are parts of the geometry model using a mouse, and then by inputting actual values. This system allows the user to enter mechanical loads in various forms for stress analysis. These loads can be concentrated forces, uniformly and nonuniformly distributed pressure, body forces. In an electrostatic analysis, the charge or voltage can be entered.

4.3 Designation of Node Density Distributions

In the present system, nodes are first generated, and then FE meshes are built. In general, it is difficult to well control element size for a complex geometry. An example of node density function is shown in Figure 6. A node density distribution over a whole geometry model is constructed as follows.

The present system stores several local node patterns such as the pattern suitable to well capture stress concentration, the pattern to subdivide a finite domain uniformly, and the pattern to subdivide a whole domain uniformly. Some of those local node patterns are selected depending on their analysis purposes, and designates their relative importance and where to locate them.

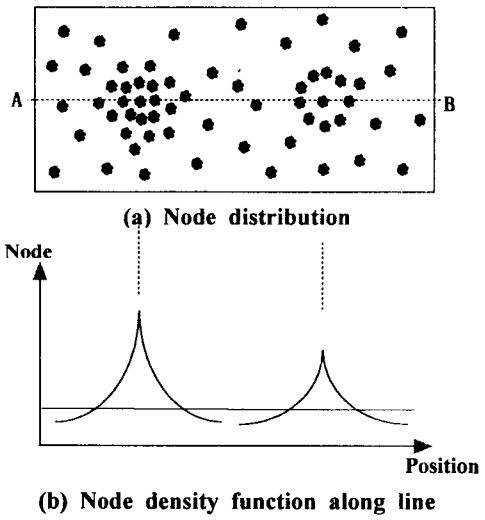

Figure 6. Example of node density function

The process is illustrated in Figure 7. For example, when either the crack or the hole exists solely in an infinite domain, the local node patterns may be regarded locally-optimum around the crack-tip or the hole. When these stress concentration sources exist closely to each other in the analysis domain, extra nodes have to be removed from the superposed region of both patterns. In the present method, a global distribution of node

density over the whole analysis domain is then automatically calculated through their superposition using the fuzzy knowledge processing[9].

4.4 Node and Element Generation

Node generation is one of time consuming processes in automatic mesh generation. Here, the advancing front method[10] is adopted to generate nodes which satisfy the distribution of node density over a whole analysis domain.

The Delaunay triangulation method[11] is utilized to generate tetrahedral elements from numerous nodes given in a geometry. If this method is utilized to generate elements in a geometry with indented shape, elements are inevitably generated even outside the geometry. However, such mis-match elements can be removed by performing the in/out check for gravity center points of such elements.

4.5 Attachment of Material Properties and Boundary Conditions to FE Mesh

Through the interactive operations mentioned in section 4.2, a user designates material properties and boundary conditions onto the geometry model. Then these are automatically attached onto appropriate nodes, edges, faces and volume of elements. Such automatic conversion can be performed owing to the special data structure of finite elements such that each part of element knows which geometric part it belongs to. Finally, a complete FE model consisting of mesh, material properties and boundary conditions is obtained.

4.6 FE Analyses

The present system automatically converts a geometry model of concern to various FE analysis models, depending on physical phenomena to be analyzed, i.e. stress analysis, modal analysis, electrostatic analysis, and so on. Then FE analyses are automatically performed.

5. Results and Disscussions

To examine mechanical and electrostatic feasibility of the present micro motor, deformation analysis of the rotor and electrostatic analysis of the air gap are performed.

5.1 In-plane Deformation Analysis of the Rotor

In-plane deformation of the rotor portion is analyzed to evaluate the quantitative relationship between a rotation angle ϕ and a torque τ_s necessary to rotate the rotor within the elastic limit of the beams. The rotor is attracted to contact with one of the electrodes through an electrostatic force. In this analysis, the displacement-controlled force with the magnitude of the distance between the rotor and one of the electrodes is applied to the rotor, considering its rotation along the inner surface of the electrodes for the purpose of simplicity. Since the electrode is much stiffer than the spiral beam, the in-plane deformation of the electrode is negligible. Thus the simplification of the loading condition employed here is quite reasonable.

Figure 7 shows a typical FE mesh, which

consists of 25,430 tetrahedral quadratic elements and 43,242 nodes. Material is assumed to be Si, and Young's modulus, E, is 190 GPa. Figure 8 shows the relationship between the calculated torque τ_s and the rotation angle ϕ. It can be seen from the figure that the rotation of the rotor is limited at about 55 degrees because of the elastic limit, i.e. 7GPa. Figure 8 also indicates that the starting torque τ_s^0 required is 0.93×10^{-8} Nm. This value of the starting torque will be referred to in the next section of electrostatic analyses.

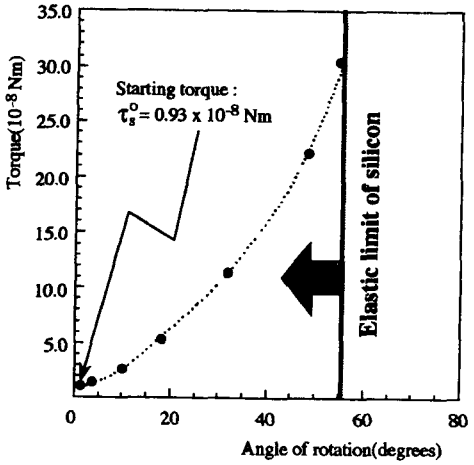

Figure 8. Calculated Torque vs. rotation angle

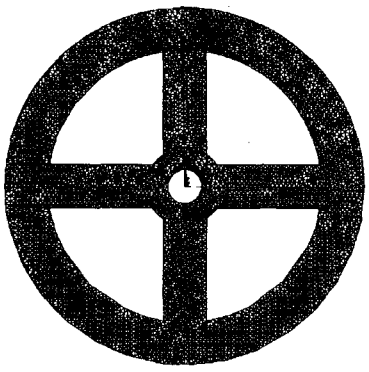

Figure 7. FE mesh of rotor

5.2 Electrostatic Analysis of Air Gap between Rotor and Stator

In general, to estimate electrostatic performances of micro actuators, in-plane two-dimensional FE analyses are often conducted because of the complexity of actual micro motor geometry. Figure 9 shows a geometry model and boundary conditions of an upper part of the air gap between the rotor and the stator. Here a sufficiently large area of the air was modeled in ordered to

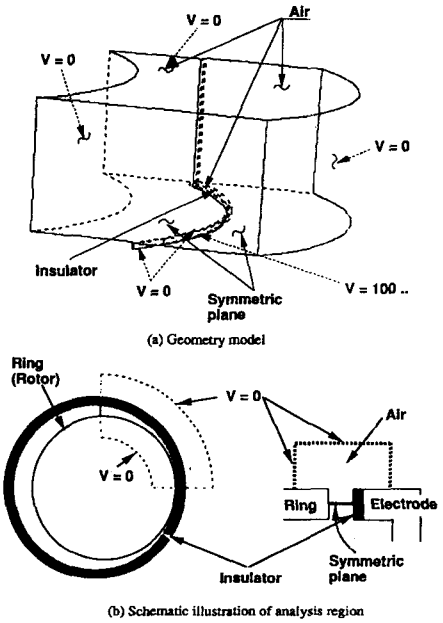

Figure 9. Geometry model and boundary condition for air gap between rotor and one of electrodes

approximately take into account infinite boundary conditions. As material properties, the permittivity of the air and insulator of SiO_2, were assumed to be 8.854×10^{12} C/Vm

and 3.542×10^{-11} C/Vm, respectively.

When one of the electrodes is excited, the rotor will be electrostatically attracted and come to contact with the insulator on the inner surface of the electrode. Then as this electrode is discharged and voltage is supplied to the next electrode, the rotor will revolve, being attracted by the excited electrode. At this moment, potential energy is stored in the capacitor formed by the rotor and the excited electrode. Figure 10 shows the calculated curves of starting torque τ_e versus driving voltage V. Here, a solid curve denotes the three-dimensional FE solutions, while the dotted curve does two-dimensional analytical solutions given in section 3. It can be seen from this figure that τ_e is proportional to V^2, and that the two-dimensional analytical solutions are two to four times larger than the three-dimensional FE ones. Such a significant difference may be caused by neglecting electrical leakage in the two-dimensional analytical solution. Considering that τ_s^0 = 0.93 $\times10^{-8}$ Nm is necessary to start rotating the rotor as given in section 5.1, it is obvious from Figure 10 that a driving voltage exceeding 210 V is indispensable in this configuration and size of the motor.

5. Conclusions

An automated FEA simulation of practical behaviors for the micro motor was performed. Deformation and electrostatic behaviors of the micro motor were effectively evaluated in an easy and consistent manner using the system developed in this study.

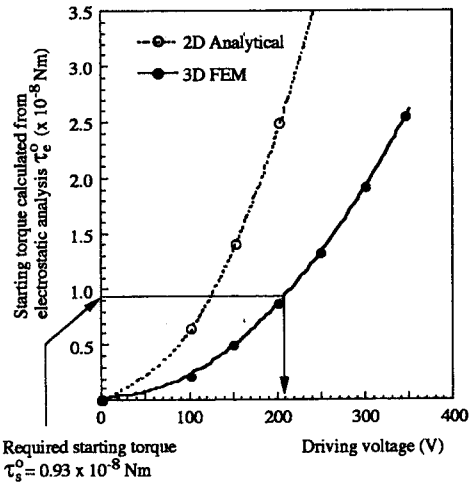

Figure 10. Calculated starting torque vs. driving voltage

Generally, three-dimensional FE modeling is required to accurately calculate the starting torque in micro motors. In this case, the starting torque obtained from the in-plane two-dimensional analytical solutions were compared with those of the actual three-dimensional FE analysis.

The starting torque is proportional to V^2, the calculated starting torque from the two-dimensional analytical solutions are three times larger than those from the three-dimensional FE solutions. It is found that the evaluation of micro motor has to be considered electrical leakage phenomenon.

References

[1] N. Nakajima, "Micromachines as Intelligent Artifacts", Proceedings of the 1st International Symposium on Research into Artifacts, Tokyo, pp. 48-51, 1993.

[2] T. Hirano, T. Furuhata, K.J. Gabriel and H. Fujita, "Design, Fabrication, and Operation of Submicron Gap Comb-Drive Microactuators", Journal of Microelectro-mechanical Systems, Vol. 1, No. 1, pp. 52- 59, 1993.

[3] S.C. Jacobsen, R.H. Price, J.E. Wood, T.H. Rytting and M. Rafaelof, "A design Overview of an Eccentric-Motion Electrostatic Micro Actuators, Sensors and Actuators, A20, pp. 1-16, 1989.

[4] R.H. Price, J.E. Wood and S.C. Jacobsen, "Modelling Considerations for Electrostatic Forces in Electrostatic Microactuators", Sensors and Actuators, A20, pp. 107-114, 1993.

[5] R. Mahadevan, "Analytical Modeling of Electrostatic Structures", in Proc. IEEE Micro Electro Mechanical Systems Workshop, pp. 120-127, 1990.

[6] Joon-Seong Lee et al.,"Automatic Mesh Generation for Three-Dimensional Constructures Consisting of Free-Form Surfaces", Journal of the Korea Society of CAD/CAM Engineers, Vol. 1, pp. 65-75, 1996.

[7] MARC Analysis Research Corporation, MARC manual k5.2, 1994.

[8] H. Chiyokura, Solid Modeling with Designbase : Theory and Implementation, Adison-Wesley, 1988.

[9] L.A. Zadeh, "Outline of a New Approach to the Analysis of Complex Systems and Decision Process", IEEE Transactions on System, Man and Cybernetics, SMC-3, pp. 28-44, 1973.

[10] E. Rank and I. Babuska, "An expert system for the optimal mesh design in the hp-version of the finite element method", Int. J. Numer. Methods Engineering, Vol. 24, pp. 2087-2106, 1987.

[11] S.W. Sloan, "A Fast Algorithm for Constructing Delaunay Triangulation in the Plane", Advances in Engineering Software, Vol. 9, pp. 162-172, 1987.

● 저자소개 ●

이준성

1986 성균관대학교 기계공학과 학사

1988 성균관대학교 기계공학과 석사

1995 The University of Tokyo 공학박사

1988~1991 육군사관학교 교수부 기계공학과 교수

1991~1992 KIST 시스템연구부 연구원

1996~현재 경기대학교 전자·기계공학부학부 부교수

관심분야: 퍼지이론, 최적화설계, 구조물 수명평가, MEMS